



MIXED CONVECTION FLOW OF A VISCOUS DISSIPATIVE AND HEAT GENERATING/ABSORBING FLUID THROUGH A SLIT MICROCHANNEL

G. Ojemer¹, A. S. Ibrahim², and I. O. Onwubuya³

¹Department of Mathematics, College of Sciences, Federal University of Agriculture, Zuru, P. M. B. 28, Kebbi State.

²Department of Mathematics, Faculty of Sciences, Sokoto State University, Sokoto State.

³Department of Mathematics, Faculty of Sciences, Air Force Institute of Technology, P. M. B. 2104, Kaduna State.

*Corresponding Author's Email: godwinojemer@gmail.com

Cite this article:

G. Ojemer, A. S. Ibrahim, I. O. Onwubuya (2024), Mixed Convection Flow of a Viscous Dissipative and Heat Generating/Absorbing Fluid Through a Slit Microchannel. African Journal of Mathematics and Statistics Studies 7(4), 87-104. DOI: 10.52589/AJMSS-LA7BTCRZ

Manuscript History

Received: 14 Aug 2024

Accepted: 17 Oct 2024

Published: 23 Oct 2024

Copyright © 2024 The Author(s). This is an Open Access article distributed under the terms of Creative Commons Attribution-NonCommercial-NoDerivatives 4.0 International (CC BY-NC-ND 4.0), which permits anyone to share, use, reproduce and redistribute in any medium, provided the original author and source are credited.

ABSTRACT: *This paper is aimed at investigating the consequences of viscous dissipation and super-hydrophobicity on a magnetized mixed convection flow of an electrically conducting fluid across an up facing microchannel influenced by a transverse magnetic field. The plates were alternatively heated and incorporated with heat source/sink effect. The modeled governing equations have been obtained using a semi-analytical (regular perturbation) method. Various line graphs have been plotted to demonstrate the behavior of key parameter dictating the flow. It was found out that the thermal gradient and fluid velocity are significantly enhanced for mounting values of mixed convection Gr_e , Brickman number Br , Darcy porous number K and heat source S parameters in the superhydrophobic microchannel for constant pressure gradient Γ . On the other hand, the velocity deteriorates for increasing levels of magnetic field M and heat sink S factors. Further, the comparison of this present analysis with previously published literature for limiting cases when $\Gamma = S = 0$ and $Gr_e = 1$ showcased an excellent concurrence, thereby confirming the accuracy and validity of this present investigation. The findings from this research will find relevance in engineering, technological and industrial processes such as for solar collectors, nuclear reactors cooled during emergency shutdown, nuclear power plants, gas turbines and the various propulsion devices for aircraft, missiles, satellites and space vehicles.*

KEYWORDS: Viscous dissipative fluid, Heat source/sink, Magnetohydrodynamics (MHD), Superhydrophobic surface (SHS), Slit Microchannel.



INTRODUCTION

Magnetic technologies are becoming more interesting in industries owing to their variety of practical applications in biomaterials for wound treatment, gastrointestinal drugs, sterilization devices and other related fields. Magneto-hydrodynamics (MHD) is one of the important areas of development in modern scientific research and engineering problem which can also be considered as a fluid mechanics sub-discipline dealing with the mutual interaction between an externally imposed magnetic field and the flows of fluids that conduct electricity (Obalalu *et al.* 2021). In transverse channel flows of incompressible liquids, the Lorentz force, rather than pump pressure, is used to accelerate the channel liquid more deeply or faster. Chemical energy technology, which includes the utilization of MHD pumps to transfer electrically conductive fluids, is currently employed in some nuclear power plants. Apart from these purposes, when the fluid is electrically conductive, an applied magnetic field can drastically boost natural convection movement (Jha *et al.*, 2015). In view of these considerations, very recently, Onwubuya and Ojmeri (2023c) presented a comparative analysis of MHD flow of a viscous and incompressible fluid traveling through a slit microchannel coated with superhydrophobic slip and temperature jump effects using homotopy perturbation method. A chemically reacting fluid that is convectively heated, hydromagnetic natural flow in a vertical channel imagined with a porous medium was investigated by Hamza *et al.* (2022). The unsteady state situation was determined using implicit finite difference scheme, while the steady-state component was solved by homotopy perturbation approach. In a separate paper, the function of MHD on natural convective slip flow of an exothermic fluid under the influence of Newtonian heating was reported by Hamza *et al.* (2021). Taid and Ahmed (2022) deliberated on the actions of the Soret effect, heat dissipation, and chemical reaction on steady two-dimensional hydro-magnetic natural convection flow across an inclined porous plate coated with porous media using the perturbation series scheme. Using the Laplace transformation procedure, Osman *et al.* (2022) described the impact of MHD on natural convection across an infinite inclined plate. Siva *et al.* (2021) outlined a detailed reaction to the MHD action on a heat transfer analysis of electroosmotic flow in a rotating microfluidic channel. Choudhary (2012) investigated heat and mass transfer problem for viscoelastic hydro-magnetic boundary layer flow toward a vertical flat plate. The scrutinization of an inclined magnetic field controlled by time-dependent natural convection of a dusty reactive fluid restricted to two infinite flat plates immersed with porous material were carried out by Sandeep and Sugunamma (2013). The effects of heat and mass transport were taken into account when Joseph *et al.* (2015) discussed time-dependent hydro-magnetic Poiseuille flow across two infinitely parallel porous plates in an inclined magnetic field. It was discovered that as the Hartman number Ha increases, velocity decreases.

Comprehending the impacts of heat generation/absorption on fluid flow patterns is extremely fundamental in several technological and physical problems of exothermic or endothermic fluid response, and these effects are key in evaluating the heat transference (Gambo *et al.*, 2021). Several scholars have investigated the effects of heat-generating/absorbing fluid on various flow regimes. In this context, Ojmeri *et al.* (2024) recently put forth an analytical study of a chemically reactive hydromagnetic fluid affected by heat generation/absorption flowing across a superhydrophobic microchannel that is heated alternatively. In addition, Ojmeri and Onwubuya (2023a) described the analysis of steady mixed convection flow of Arrhenius-controlled chemical reaction and an exothermic fluid along an isothermally heated superhydrophobic microchannel due to heat source/sink. In another paper, Ojmeri and Hamza (2022) presented a theoretical investigation of a chemically reactive fluid in a MHD natural



convection flow blended with heat source and sink effects employing homotopy perturbation approach. They concluded that raising the viscous heating parameter significantly encourages the fluid motion and the volume flow rate respectively. Oni and Jha (2019) investigated the effects of a heat source and sink fluid on natural convection confined to an upstanding annulus with time-periodic heating boundary conditions. They discovered that heat generation and absorption parameters affect velocity distribution, periodic temperature profile, Nusselt number, and frictional force at the cylinder walls, respectively. Gambo and Gambo (2020) extensively scrutinized the effects of fully developed natural convective flow of heat generating/absorbing fluid in an open-ended vertical concentric annulus with a magnetic field effect. Their findings show that by carefully selecting appropriate values for the heat generation or absorption parameter and the Hartmann number, they may be used to control the temperature and velocity profiles. Chu *et al.* (2020) investigated the nonlinear thermal radiation and heat sink/source of a bidirectional periodically moving surface driven flow in a rate type nanofluid containing a gyrotactic microbe. Zhao *et al.* (2021) highlighted the effects of heat generation/absorption, dissipation, radiative heat flux and joule heating on the mixed convective entropy optimized nanomaterial MHD flow of Ree-Eyring fluid formed by two rotating disks. The consequences of thermal radiation, a heat source, and an induced magnetic field on the natural convective flow of a couple stress fluid in a flux-isothermal vertical channel have been evaluated by Hasan *et al.* (2020) using the method of an indeterminate coefficient. Parthiban and Pasad (2023) outlined a theoretical investigation of radiative-convection effects on MHD fluid flow in a heated square enclosure having a non-Darcy square cavity in the coexistence of the Hall effect and the heat source or sink.

Microchannel studies are very relevant because of the ever-increasing needs for size reductions and analysis of components' performances for optimum results in the micro-electro-mechanical systems (MEMS) industry. Investigations such as those carried out by Thakre *et al.* (2008) and Tamilselvan *et al.* (2018) shed more lights on this. Scientists, technicians, and engineers are eager to see how the unique combination of hydro-magnetic free convection in a super-hydrophobic (SHO) micro-channel performs. Because of the enormous slip obtained from liquid/solid interfaces, SHO surfaces have the ability to reduce drag in a flow, making it a particularly relevant parameter to gauge the extent of drag reduction depending on the slip length in oil and gas companies, semiconductor manufacturing facilities, and companies that assemble small equipment. With these concerns in mind, Ojemeru and Onwubuya (2023b) recently described the combined effects viscous dissipation and Darcy porous medium on MHD free convection flow through a microchannel that is equipped with a superhydrophobic slip and temperature jump conditions. They concluded from their findings that superhydrophobicity effect encourages the fluid velocity in the microchannel for mounting level of viscous dissipative parameter. Yale *et al.* (2023) investigated the impacts of superhydrophobicity and MHD on a viscous dissipative fluid in a slit microchannel coated with a superhydrophobic surface using a regular perturbation approach. Wang and Ng (2014) explored the role of isothermal and iso-flux heating conditions on natural convection in a slit micro-channel. Jha and Gwandu (2017) extended Wang and Ng's (2014) work by conducting a theoretical study of hydro-magnetic natural convection in a vertical slit micro-channel having super-hydrophobic slip and temperature jump. When there is a temperature leap and no superhydrophobic slip, or both, the maximal upward velocity obtained by heating the superhydrophobic surface is less than that obtained by heating the no-slip surface. When neither is present, the maximum velocities are similar. Later again, Jha and Gwandu (2019) used non-linear Boussinesq approximation methods to examine free convection of an electrically



conducting fluid in a vertical slit micro-channel coated with super-hydrophobic slip and temperature jump conditions. According to the computational results, increasing the temperature jump coefficient contributes to a decrease in temperature when the super-hydrophobic surface is heated and an increase in temperature when the no-slip surface is heated. In another paper, Jha and Gwandu (2020) offered another study of free convection airflow through porous plates heated alternately, one with no slip and the other super-hydrophobic. Ramanuja *et al.* (2020) evaluated free convection flow in an isothermally heated channel with super-hydrophobic slip on one surface and a temperature rise, but no slip on the other. Hatte and Pitchumani (2021) extensively and explicitly described the impact of heat transfer flow within a cylinder having no wetting surfaces using a fractional rough surface characterization. The method investigates the fluid interaction's dynamic stability in the asperities of air-infused super-hydrophobic surfaces. Their results show that, contrary to what most people think, super-hydrophobicity, which is defined by the highest contact angles, does not always lead to peak convective heat transfer behavior and that, under some fluid flow situations, hydrophobic surfaces can give high thermal performance.

From the preceding discourse, not much attention has been devoted to the investigation of magnetized mixed convection flow with heat source/sink effects on an alternately heated slit microchannel. Hence, to bridge the knowledge gap found in this literature, the main purpose of this article is to build on the work of Ojemeru and Onwubuya (2023b) by performing a theoretical investigation of magnetized mixed flow influenced by heat source/sink effect across a slit microchannel that is alternately heated and equipped with superhydrophobic slip and temperature jump conditions. The modelled dimensionless governing equations are a set of coupled ordinary differential equations which has been solved semi-analytically by regular perturbation. Illustrative graphs have been also sketched to demonstrate the impacts of embedded parameters dictating the flow configuration. The results of this study can find applicability in areas such as cooling of nuclear reactors and energy efficient drying processes. Additionally, this study can provide wider applications into mechanical micro-fluidics, micro-electro mechanical systems (MEMS), microelectronics and bio-fluidics than the previous related studies available in the literature. Because of the enormous slip obtained from liquid/solid interfaces, SHS have the capacity to minimize drag in a flow, making it a very useful parameter for evaluating the extent of drag reduction based on the slip length in oil and gas companies, semiconductor fabricating facilities, and companies that assemble small equipment.

Problem Formulation

Imagine an electrically-conducting fluid moving steadily upward through a vertical parallel plate micro-channel by mixed convection through heating one of the plates at a time. One of the surfaces is extremely difficult to wet (super-hydrophobic) as a result of a special micro-engineering treatment. The other side (no-slip surface) was not tempered with. The super-hydrophobic surface is kept at a position $y_0 = 0$ while the no-slip surface is at $y_0 = L$, as shown by Figure 1. Different temperature jump and slip conditions were used for the different plates because the main interest is in the super-hydrophobicity of a surface, not the characteristics of the flow. A magnetic field of uniform strength $(0, B_0, 0)$ is assumed to be applied in the direction perpendicular to the direction of flow. Heat flow along the channel was neglected. Following Ojemeru and Onwubuya (2023b) under the Boussinesq buoyancy approximation and assuming that the fluid is viscous, electrically conducting, and in the presence of sink/source, the controlling equations for the present problems in dimensional form can be as follows:

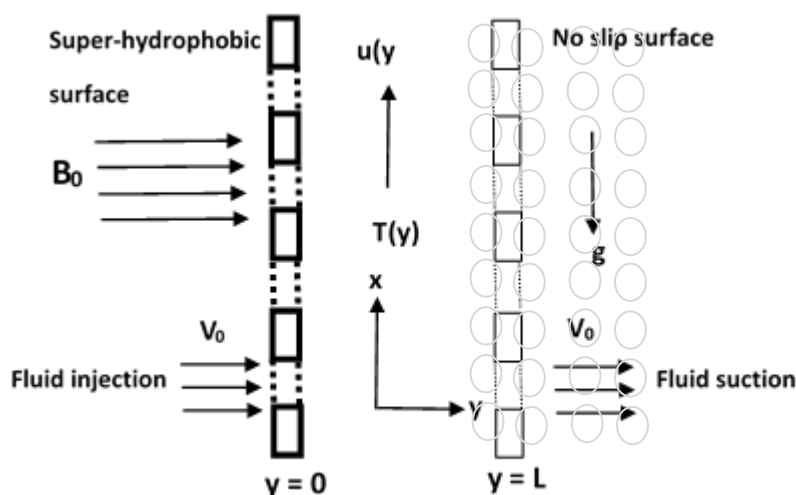


Figure 1: Physical Coordinate of the Flow System

$$v \frac{d^2 u'}{dy'^2} + g \beta (T' - T_0) - \frac{\sigma B_0^2 u'}{\rho} - \frac{u'}{K} = \frac{1}{\rho} \frac{dP}{dX} \tag{1}$$

$$\frac{k}{\rho c_p} \frac{d^2 T'}{dy'^2} + \frac{v}{c_p} \left[\left(\frac{\partial u'}{\partial y'} \right)^2 \right] - \frac{Q(T' - T_0)}{\rho c_p} = 0 \tag{2}$$

We assume that the appropriate boundary conditions at the walls are:

$$\left. \begin{aligned} u(y') &= \lambda' \frac{du'}{dy'} \\ T(y') &= T_0 + A(T_h - T_0) + \gamma' \frac{dT'}{dy'} \end{aligned} \right\} \text{at } y' = 0 \tag{3}$$

$$\left. \begin{aligned} u(y') &= 0 \\ T(y') &= T_0 + B(T_h - T_0) \end{aligned} \right\} \text{at } y' = L$$

Closed Form Solution

To solve Eqns (1) to (3), we employ the dimensionless quantities and parameters:

$$u = \frac{u'}{U}, y = \frac{y'}{h}, \theta = \frac{T' - T_0}{T_w - T_0}, x = \frac{x'v}{Uh^2}, M^2 = \frac{\sigma \beta_0^2 h^2}{\rho v}, (Y, \gamma, \lambda) = (Y', \gamma', \lambda')/h$$

$$S = \frac{Q_0 h^2}{k}, Br = EcPr, Gr = \frac{g \beta (T_1' - T_0) x^3}{v^2}, Re = \frac{U_0 x}{v}, \Gamma = \frac{1}{\rho} \frac{\partial P}{\partial x}, \text{ where and} \tag{4}$$

Using the dimensionless quantities in Eqn (4), the basic Eqns (1) to (3) become:



$$\frac{d^2U}{dy^2} - \left(M^2 + \frac{1}{K}\right)U + \frac{Gr}{Re}\theta = \Gamma \quad (5)$$

$$\frac{d^2\theta}{dy^2} + Br \left(\frac{du}{dy}\right)^2 - S\theta = 0 \quad (6)$$

The initial and boundary conditions in dimensionless forms are:

$$\theta(Y) = 1 + \gamma \frac{d\theta}{dY} \quad U(Y) = \lambda \frac{dU}{dY} \quad \text{at } Y = 0 \quad \theta(Y) = 1 \quad U(Y) = 0 \quad \text{at } Y = 1 \quad (7)$$

where M is the magnetic field intensity, $\frac{Gr}{Re}$ is the mixed convection parameter, Γ is the constant pressure gradient, $Br = EcPr$ is the Brinkman number, S is the heat source/sink parameter, K is the permeability parameter, Γ is the temperature jump coefficient and λ is the velocity slip condition.

$$\text{We assume that } \theta = \theta_o + Br\theta_1 \quad U = U_o + BrU_1 \quad (8)$$

Substituting U & θ into equation (5) to (7) and comparing the coefficient according to B_r^o & B_r , we have

$$B_r^o: \frac{d^2U_o}{dy^2} + \frac{Gr}{Re}\theta_o - M^2U_o = \Gamma \quad (9)$$

$$B_r: \frac{d^2U_1}{dy^2} + \frac{Gr}{Re}\theta_1 - M^2U_o = 0 \quad (10)$$

$$\begin{aligned} B_r^o: \frac{d^2\theta_o}{dy^2} - S\theta_o \\ = 0 \end{aligned} \quad (11)$$

$$\begin{aligned} B_r: \frac{d^2\theta_1}{dy^2} + \left(\frac{du_o}{dy}\right)^2 - S\theta_1 \\ = 0 \end{aligned} \quad (12)$$

The transformed boundary conditions become

$$\begin{aligned} U_o = \lambda \frac{dU_o}{dy} \quad U_1 = \lambda \frac{dU_1}{dy} \quad \text{at } y = 0 \quad U_o = 0 \quad U_1 = 0 \quad \text{at } y \\ = 1 \end{aligned} \quad (13)$$

$$\begin{aligned} \theta_o = 1 + \gamma \frac{d\theta_o}{dy} \quad \theta_1 = \gamma \frac{d\theta_1}{dy} \quad \text{at } y = 0 \quad \theta_o = 1 \quad \theta_1 = 0 \quad \text{at } y = 1 \end{aligned} \quad (14)$$

The analytical solutions of the temperature and velocity is derived as:

$$\theta_o = A_1y + A_2 \quad (15)$$

$$U_o = A_3e^{Ry} + A_4e^{-Ry} + A_5y + A_6 \quad (16)$$



$$\theta_1 = -\frac{b_1}{4R^2} e^{2Ry} - \frac{b_2}{R^2} e^{Ry} - \frac{b_3}{R^2} e^{-Ry} - \frac{b_4}{4R^2} e^{-2Ry} - b_5 \frac{y^2}{2} + A_7 y + A_8 \quad (17)$$

$$U_1 = B_1 e^{Ry} + B_2 e^{-Ry} + B_3 e^{2Ry} + B_4 y e^{Ry} + B_5 y e^{-Ry} + B_6 e^{-2Ry} + B_7 y^2 + B_8 y + B_9 \quad (18)$$

Recall that

$$\theta = \theta_0 + B_r \theta_1 \text{ and}$$

$$U = U_0 + B_r U_1$$

The rates of heat transfer and skin frictions at both plates are obtained as follows:

$$\frac{d\theta}{dy} \Big|_{y=0} = A_1 + B_r \left[-\frac{b_1}{2m} - \frac{b_2}{m} + \frac{b_3}{m} + \frac{b_4}{2m} + A_7 \right] \quad (19)$$

$$\frac{d\theta}{dy} \Big|_{y=1} = A_1 + B_r \left[-\frac{b_1}{2m} e^{2m} - \frac{b_2}{m} e^m + \frac{b_3}{m} e^{-m} + \frac{b_4}{2m} e^{-2m} - b_5 + A_7 \right] \quad (20)$$

$$\frac{dU}{dy} \Big|_{y=0} = A_3 m - A_4 m + A_5 + B_r [B_1 m e^{my} - B_2 m e^{-my} + 2B_3 m e^{2my} + B_4 m y e^{my} + B_4 e^{my} - B_5 m y e^{-my} + B_5 e^{-my} - 2m B_6 e^{-2my} + 2B_7 y + B_8] \quad (21)$$

$$\frac{dU}{dy} \Big|_{y=1} = A_3 m e^m - A m e^{-m} + A_5 + B_r [B_1 m e^m - B_2 m e^{-m} + 2B_3 m e^{2m} + B_4 m e^m + B_4 e^m$$

$$+ B_5 m e^{-m} + B_5 e^{-m} - 2B_6 m e^{-2m} + 2B_7 + B_8] \quad (22)$$

RESULTS AND DISCUSSION

This section is devoted to evaluating the impacts of porous medium on steady MHD mixed flow of an electrically-conducting heat generating/absorbing fluid, moving upward through an isothermally heated parallel plate micro-channel, with one surface having super-hydrophobic slip condition and temperature jump, while the other has no slip. The flow is influenced by a constant pressure gradient. The steady state leading equations are solved analytically using regular perturbation series method. Various graphs were plotted with the help of a user-friendly software program to showcase the effects of controlling parameters on the fluid flow and thermal gradient. The implication of the Brickman number (Br) on the dimensionless temperature for fixed value of ($\lambda = \gamma = 1$) is displayed in Figure 4.1. It clearly reveals that, from this figure, the temperature of the fluid increases with an increase in the local Brickman number (Br) significantly. Higher Brickman numbers mean correspondingly higher degrees of convective heating at the lower channel wall and consequently lead to high temperature at the lower plate. The influence of the Brickman number (Br) on the dimensionless velocity profile for fixed value of $\lambda = \gamma = 1$ is displayed in Figure 4.2. It seems that, from this figure, the velocity of the fluid increases with an increase in the local Brickman number (Br) significantly. Higher Brickman numbers mean correspondingly higher degrees of convective heating at the lower channel wall and consequently lead to high velocity at the cold plate. With the aid of Figure 4.3, we comprehend the behavior of fluid velocity as the mixed convection parameter



is varied. It is apparent from this figure that the fluid velocity accelerates as the porosity parameter is increased. We observe that, with the growth in permeability of the porous medium, the drag force weakens; because of this, the velocity gradient of the fluid improves. Moreover, this makes sense because when a lot of fluid is moved, more viscous energy is produced. This causes the fluid boundary wall and thickness to grow, which speeds up the movement of the fluid. Figures 4.4a and 4.4b demonstrate the influence of a heat source or sink parameter on the thermal fluid. A close examination at these figures reveals that the temperature is expanded for $S < 0$, as shown in Figure 4.4a, but the temperature is contracted for $S > 0$, as shown in Figure 4.4b. With heat generation along the cold wall, greater thermal profiles are envisaged. This is physically accurate because when heat is absorbed, the fluid becomes denser and the convection current weakens, resulting in a fall in fluid temperature. Increased heat generation, on the other hand, intensifies the convection current, resulting in a fall in fluid density and a rise in temperature. Figures 4.5a and 4.5b show the effects of changing the heat source or sink settings on the velocity gradient. Similarly, as expected, the same effects seen in the temperature gradient are duplicated in the fluid velocity when the heat source ($S < 0$) and heat sink ($S > 0$) levels increase. Naturally speaking, this can be attributed to the additional heat boost, which amplifies the heat flow characteristics of the system, resulting in an increase in the thermal profile of the fluid and therefore improving flow in the system. In addition, heat source/sink parameter is thought to contain more heat near the plate, which helps the fluid travel faster and so extends the fluid's velocity and temperature inside the boundary layer region. Also, the thickness of the thermal and momentum boundary walls rose in the micro-channel as the internal heat generation or absorption parameter increased. Figure 4.6 demonstrates the action of MHD on the velocity distribution. The pattern shows reduction in upward velocity (especially the peak velocity) with increase in magnetic field strength (when both λ and γ are each equal to 1).

The actions of Brickman number (Br) on the rate of heat transfer coefficient are displayed respectively in Figure 4.7. The rate of heat transfer is high when Br is large, while the increasing time leads to reduction in the rate of heat transfer (See Figure 4.7a (at $y=0$)). A reverse trend is observed in Figure 4.7b (at $y=1$). The actions of Brickman number (Br) on wall shear stress coefficient is displayed in Figure 4.8. It is shown from Figure 4.8a that the fictional factor is stronger at $y=0$ when the Brickman number is enhanced while an opposite phenomenon is witnessed at $y=1$ as portrayed in Figure 4.8b.

The variations of heat source/sink on the skin friction and rate of heat transfer is displayed in Figures 4.9–4.12. In Figure 4.9, it is revealed that raising the heat generation parameter leads to an upsurge in the heat transfer rate at $y=0$, while a reverse situation is observed at $y=1$. As seen in Figure 4.10, a diminishing effect is noticed for the increasing function of the heat absorption parameter at the lower plate, whereas an opposite case occurs at the upper plate. A similar trend as demonstrated on heat transfer rate is also observed on the skin friction for deviations of heat generation/absorption at both plates, as shown in Figures 4.11a and 4.11b. A decreasing tendency is also observed on the skin friction for deviations of heat generation/absorption at both plates, as shown in Figures 4.12a and 4.12b.

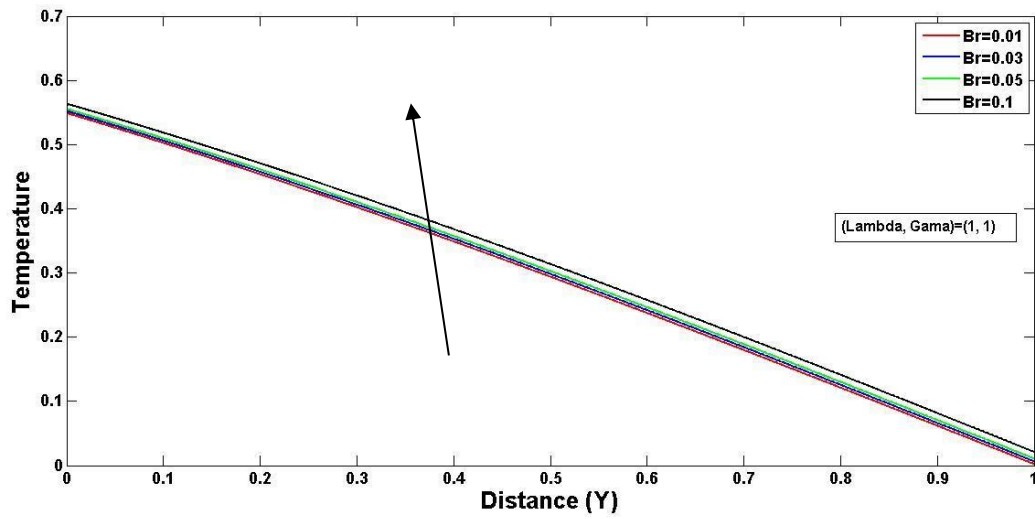


Figure 4.1: Deviation of Br on temperature gradient

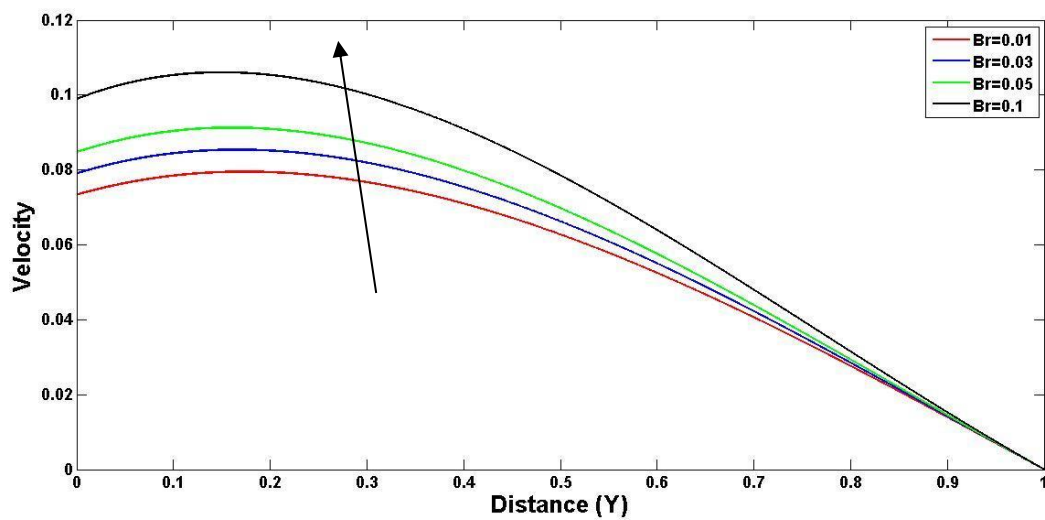


Figure 4.2: Deviation of Br on velocity gradient

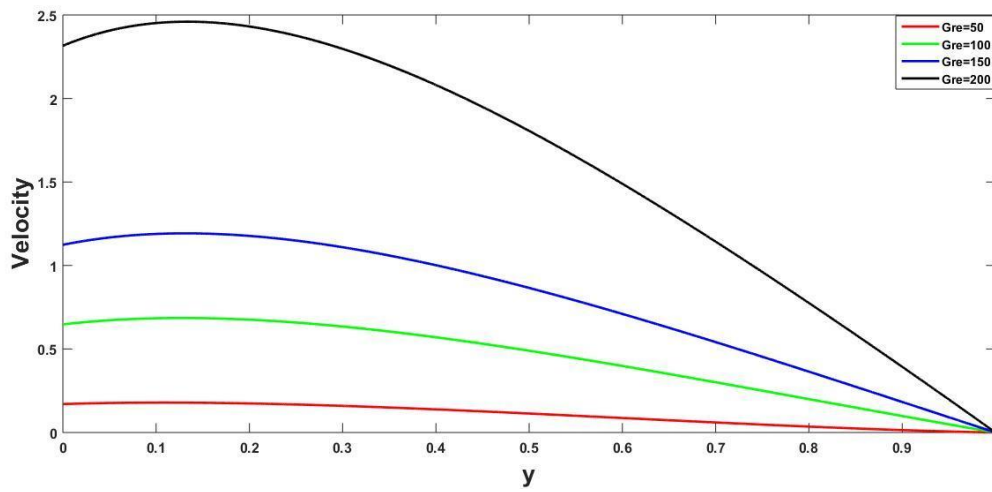


Figure 4.3: Deviation of Gre on velocity gradient

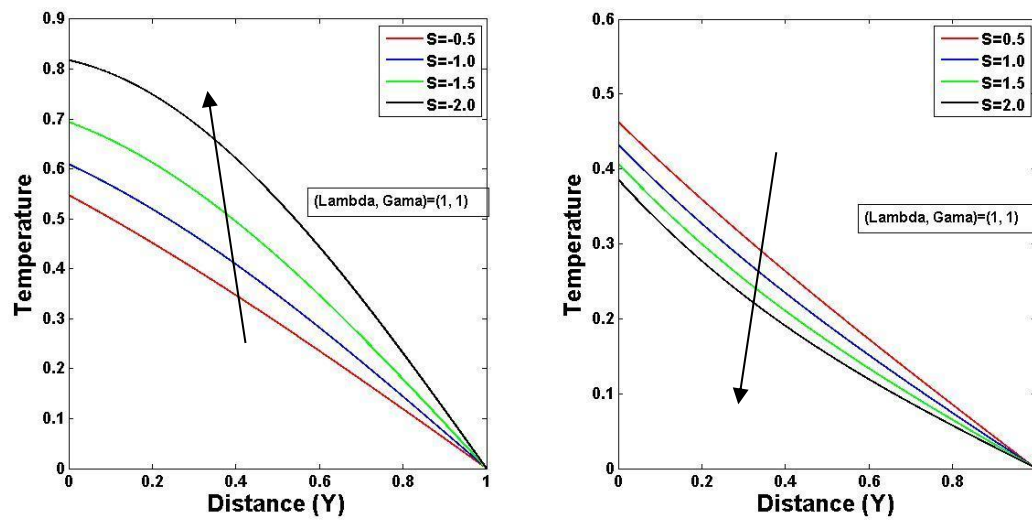


Figure 4.4: Deviation of heat source/sink on temperature gradient

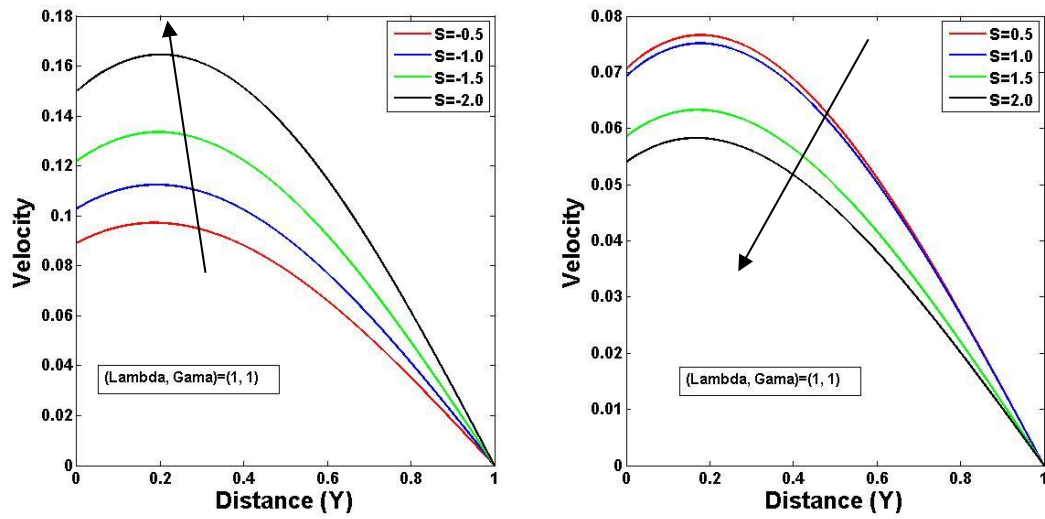


Figure 4.5: Deviation of heat source/sink on velocity gradient

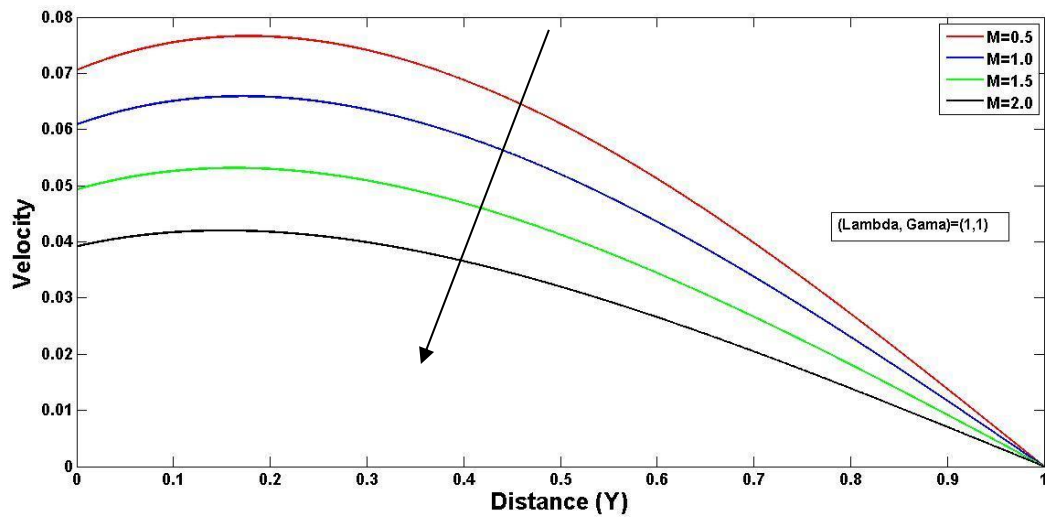


Figure 4.6: Deviation of M on velocity gradient

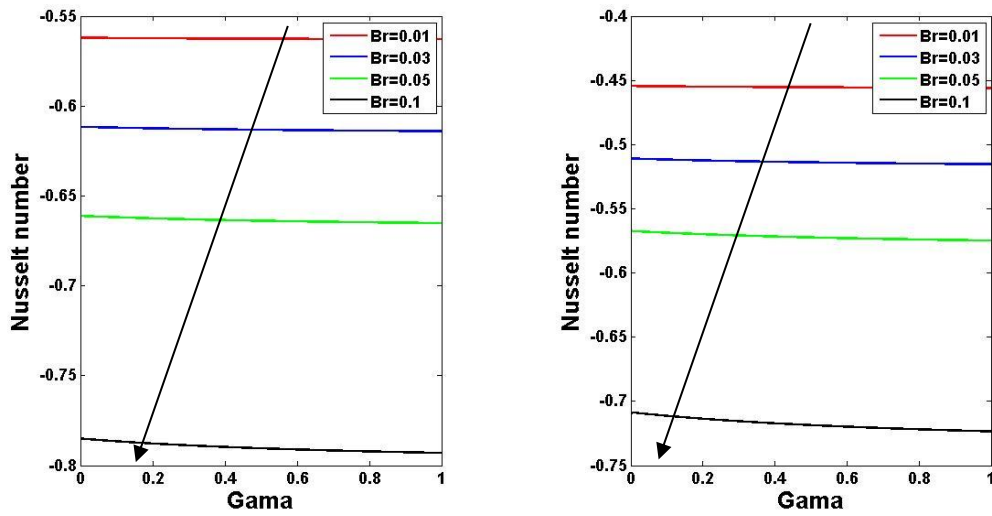


Figure 4.7: Deviation of Br on Nusselt number

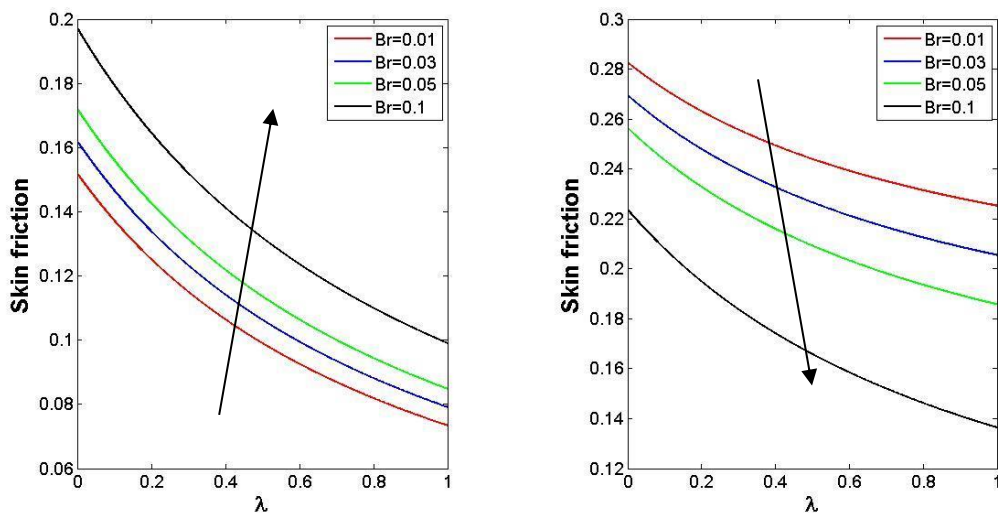


Figure 4.8: Deviation of Br on skin friction

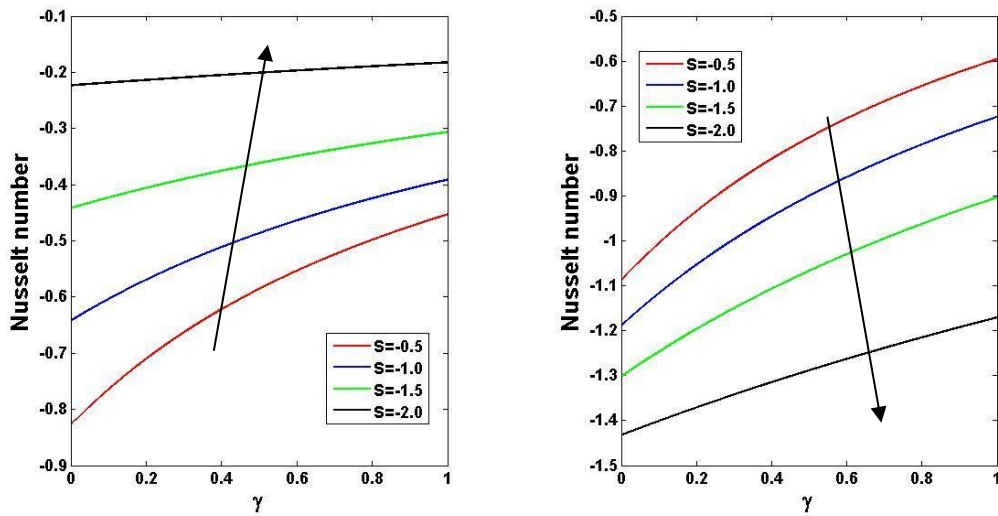


Figure 4.9: Deviation of heat source on Nusselt number

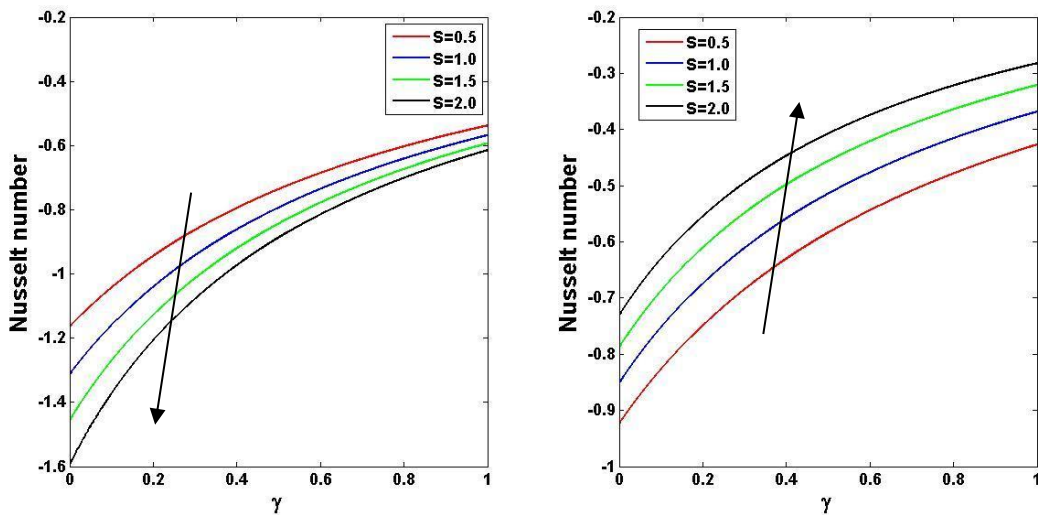


Figure 4.10: Deviation of heat sink on Nusselt number

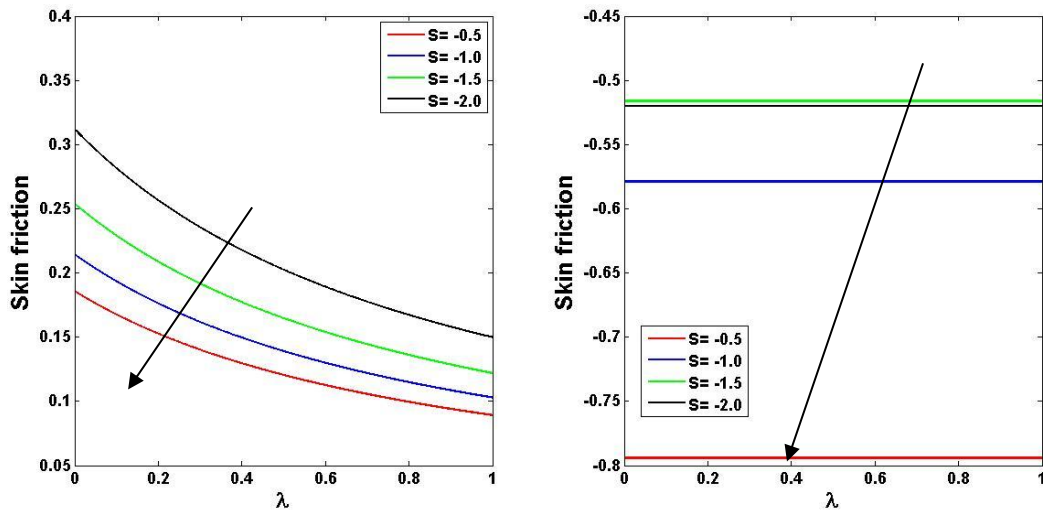


Figure 4.11: Deviation of heat source on skin friction

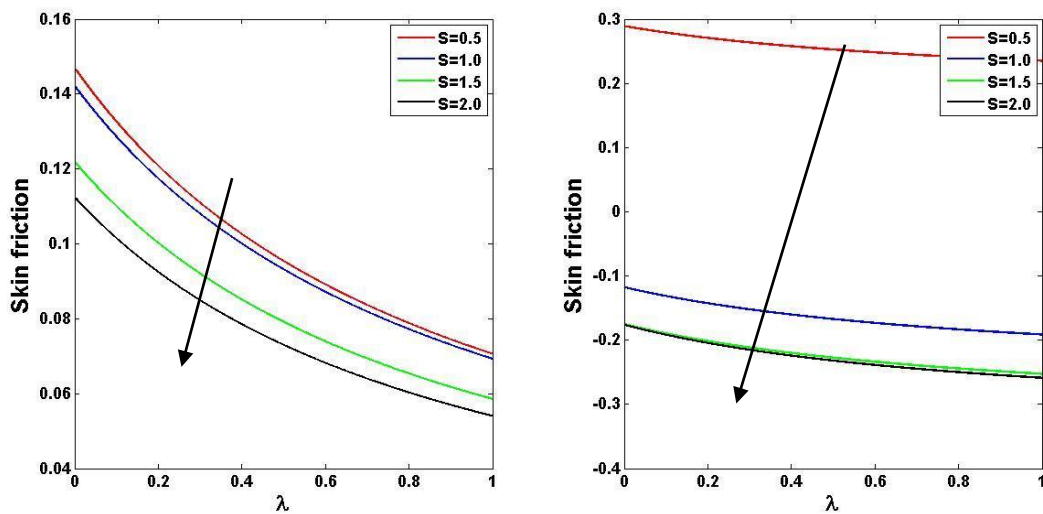


Figure 4.12: Deviation of heat sink on skin friction



VALIDATION OF RESULTS

The work of Ojemeru and Onwubuya (2023b) is successfully recovered by setting $\Gamma = S = 0$ and $Gre = 1$.

Table 1: Numerical comparison between the work of Ojemeru and Onwubuya (2023b) with the present study for temperature and velocity profiles for $\lambda = \gamma = 1$, $M = 0.5$ when $\Gamma = S = 0$ and $Gre = 1$

Y	Ojemeru and Onwubuya (2023b)	Present work		
	$\theta(Y)$	U(Y)	$\theta(Y)$	U(Y)
0.1	0.4500	0.0843	0.4500	0.0843
0.2	0.4000	0.0856	0.4000	0.0856
0.3	0.3500	0.0831	0.3500	0.0831
0.4	0.3000	0.0772	0.3000	0.0772
0.5	0.2500	0.0686	0.2500	0.0686

CONCLUSION

This paper inspected the impact of permeability factor on a steady fully developed hydromagnetic flow of an electrically conducting fluid, moving vertically through an isothermally heated porous plates micro-channel with one plate exhibiting super-hydrophobic slip and temperature jump, while the other did not. Since the governing equations are a system of ordinary differential equations with constant coefficients, a closed form solution has been obtained by using a semi-analytical method. The impacts of controlling parameters such as porous medium, Brinkman number, heat source/sink and magnetic field intensity on the fluid flow, temperature, drag force and heat transfer amount were presented and discussed fully with the help of illustrated plots. The summary of the noteworthy findings are as follows:

- i. The fluid velocity and the thermal gradient increase with an increase in the Brinkman number parameter but the local skin friction is reduced at $y=0$ while the reverse phenomenon occurs at $y=1$.
- ii. The mixed convection parameter is seen to enhance the fluid velocity in the superhydrophobic microchannel for constant pressure gradient.
- iii. The velocity of the fluid is lowered with an increase in the magnetic field while the skin friction is higher at $y=0$ than at $y=1$.
- iv. When $S>0$, which represents heat absorption, the fluid velocity and the temperature gradients respectively are seen to rise significantly, whereas for $S<0$, which denotes heat emission, a reverse phenomenon occurs.
- v. The rate of heat transfer is higher at the plate $y=1$ while a reverse trend is observed at $y=0$ for growing values of Br .



- vi. The frictional force is seen to be enhanced for increasing values of heat generation parameter at $y=0$, whereas a reverse case is recorded at $y=1$.
- vii. The heat absorption parameter is to strengthen the sheer stress at $y=0$, while an opposite phenomenon situation is noticed at $y=1$.

REFERENCES

- Chaudhary, D. (2012). Heat and Mass Transfer for visco-elastic MHD Boundary Layer Flow Past a Vertical Plate, *Theoretical Applications in Mechanics*, **33**, pp. 281-309.
- Chu Y., Aziz S., Ijaz K. M., Khan S. U., Nazeer M., Ahmad I. and Tlili, I. (2020). Nonlinear radiative bioconvection flow of Maxwell nanofluid configured by bidirectional oscillatory moving surface with heat generation phenomenon, *Physica Scripta* vol 95(10). <https://doi.org/10.1088/1402-4896/abb7a9>
- Fakour M., Vahabzadeh A. and Ganji D. D. (2015). Study of heat transfer and flow of nano-fluid in permeable channel in the presence of magnetic field. *Propulsion and Power Research*, 4, 50–62.
- Gambo D., Yusuf, T. S., Oluwagbemiga, S. A., Kozah, J. D. and Gambo J. J. (2021). Analysis of free convective hydromagnetic flow of heat generating/absorbing fluid in an annulus with isothermal and adiabatic boundaries. *Partial Differential Equations in Applied Mathematics*. <https://doi.org/10.1016/j.padiff.2021.100080>
- Gambo J. and Gambo D. (2020). On the effect of heat generation/absorption on magneto-hydrodynamic free convective flow in a vertical annulus: An Adomian decomposition method. *Heat transfer*, Wiley. 50(1), 1-15. DOI: 10.1002/hti.21978.
- Hamza, M. M., Bello, I., Mustapha, A., Usman, U. and Ojemer, G. (2023). Determining the role of thermal radiation on hydro-magnetic flow in a vertical porous super-hydrophobic microchannel, *Dutse Journal of Pure and Applied Sciences*, 9(2b), pp. 297-308.
- Hasan, N. Z. Mohammed, Y. Nasreen, S. N. (2020). Effects of thermal radiation, heat generation and induced Magnetic field on Hydromagnetic free convective flow of couple stress fluid in an isoflux-isothermal vertical channel, *Journal of Applied Mathematics*, vol.2020, Article ID 4539531.
- Hatte, S., and Pitchumani, R. (2021). Analysis of convection heat transfer on multiscale rough super-hydrophobic and liquid infused surfaces, pp. 1-29. <https://www.sciencedirect.com/science/article/am/pii/S13858947210184>
- Jha, B. K and Gwandu, B. J. (2017). MHD free convection flow in a vertical slit micro-channel with super-hydrophobic slip and temperature jump: Heating by constant wall temperature, *Journal of Alexandria Engineering*, 57(3), pp. 2541- 2549.
- Jha, B. K. and Gwandu, B. J. (2019). MHD free convection flow in a vertical slit micro-channel with super-hydrophobic slip and temperature jump: non-linear Boussinesq approximation approach, *SN Applied Sciences*, DOI: 10.1007/S42452-019-0617-Y.
- Jha, B. K., and Gwandu, B. J. (2020). MHD free convection flow in a vertical porous super-hydrophobic microchannel, *Journal of Process Mechanics Engineering*, **235**(2), pp 1-13.
- Jha, B. K., Azeez, L. A., and Oni, M. O. (2019). Unsteady Hydromagnetic-Free convection flow with suction/injection. *Journal of Taibah University*, 13, pp.136–145.
- Joseph, K. M., Ayuba, P., Nyitor, L. N., and Muhammed, S.M. (2015). Effect of Heat and Mass Transfer on Unsteady MHD Poiseuille flow between Two Infinite Parallel Porous plates



- in an Inclined Magnetic Field, *International Journal of Scientific Engineering and Applied Sciences*, **1**(5), pp. 1-14.
- Nayak A, Dash G. C. and Panda S. (2013). Unsteady MHD flow of a visco-elastic fluid along vertical porous surface with chemical reaction. *Proceedings National Academic Sciences*, **83**, pp. 153–161.
- Obalalu A. M., Ajala O. A., Adeosun A. T., Aindele A. O., Oladapo O. A. and Olajide O. A. (2021). Significance of variable electrical conductivity on non-Newtonian fluid flow between two vertical plates in the coexistence of Arrhenius energy and exothermic chemical reaction, *Partial Differential Equations Applications and Mathematics*, **4**, 100184, pp. 1-9
- Ojemeru G. and Onwubuya I. O. (2023a). Analysis of mixed convection flow on Arrhenius-controlled heat generating/absorbing fluid in a superhydrophobic microchannel: A semi-analytical approach, *Dutse Journal of Pure and Applied Sciences*, **9**, 344-357. DOI:104314/dujopas.v9i2a.34
- Ojemeru G. and Onwubuya I. O. (2023b). Significance of viscous dissipation and porosity effects in a heated superhydrophobic microchannel, *Journal of Engineering and Technology (JET)*, **14**(2), 1-19.
- Ojemeru, G. and Hamza, M. M. (2022). Heat transfer analysis of Arrhenius-controlled free convective hydromagnetic flow with heat generation/absorption effect in a microchannel, *Alexandria Engineering Journal*, **61**, pp. 12797-12811. DOI: 10.1016/j.aej.2022.06.58
- Ojemeru, G., Onwubuya I. O., Omokhuale, E., Hussaini A. and Shuaibu, A. (2024). Analytical investigation of Arrhenius kinetics with heat source/sink impacts along a heated superhydrophobic microchannel, *UMYU Scientifica*, **3**(1), 61-71. DOI:105619/usci.2431.004
- Oni M. O. and Jha B. K. (2019). Heat generation/absorption effect on natural convection flow in a vertical annulus with time-periodic boundary conditions. *Journal of Aircraft and Spacecraft Technology*, **3**(1), 183-196. <https://doi.org/10.3844/jastsp.2019.183.196>
- Onwubuya I. O. and Ojemeru G. (2023c). Evaluation of mixed convection-radiation flow of a viscous fluid restricted to a vertical porous channel: A comparative Study, *Caliphate Journal Science and Technology*, **5**(3), pp. 1-9.
- Osman H. I, Omar N. F. M., Vieru D. and Ismail Z. (2022). A study of MHD free convection flow past an infinite inclined plate, *Journal of Advances in Research of fluid Mechanics and Thermal Sciences*, **92** (1), pp. 18-27.
- Parthiban S. and Prasad V. R. (2023). Thermal radiation and Hall current effects in a MHD non-Darcy flow in a differentially heated square enclosure Lattice-Boltzmann simulation. *Journal of Porous Media*, Begell house, **26**(5), pp37-56. DOI: 10.1615/JPorMedia.2022044054.
- Ramanuja, M., Krishna, G. G., Sree, H. K., Radhika, V. N. (2020). Free convection in a vertical slit microchannel with super-hydrophobic slip and temperature jump conditions, *International Journal of Heat Technology*, **38**(3), pp. 738-744.
- Sandeep, N. and Sugunamma, V. (2013). Effect of an Inclined Magnetic Field on Unsteady free convection flow of a dusty viscous fluid between two Infinite flat Plates filled by a Porous medium, *International Journal of Applied Mathematics and Modelling*, **1**(1), pp. 16-33.
- Siva, T., Jaangili, S. and Kumbhakar, B. (2021). Heat transfer analysis of MHD and electroosmotic flow of non-Newtonian fluid in a rotating microfluidic channel: an exact solution, *Applications of Mathematics and Mechanics*, **42**, pp. 1047-1062.



- Taid, B. K. and Ahmed, N. B. (2022). MHD free convection flow across an inclined porous plate in the presence of heat source, solet effect and chemical reaction affected by viscous dissipation ohmic heating, *Bio-interface Research in Applied Chemistry*, **12**(5), pp. 6280-6296.
- Tamilselvan V, Jayabarathi T, Raghunathan T, et al. (2018). Optimal capacitor placement in radial distribution system using flower pollination algorithm. *Alexandria Engineering Journal*, **57**, pp. 2775–2786
- Thakre K, Mohanty KB and Chatterjee A. (2018). Reduction of circuit devices in symmetrical voltage source multilevel inverter based on series connection of basic unit cells. *Alexandria Engineering Journal*, **57**, pp. 2703–2712.
- Wang, C. Y. and Ng C-O. (2014). Natural convection in a vertical slit micro-channel with super-hydrophobic slip and temperature jump. *ASME Journal of heat transfer*, **136**, 034502.
- Yale I. D., Uchiri A. M. T., Hamza M. M., and Ojemer G. (2023). Effect of viscous dissipation fluid in a slit microchannel with heated superhydrophobic surface, *Dutse Journal of Pure and Applied Sciences*, **9**(3b), pp. 290-302.
- Zhao T., Khan M. and Chu Y. (2020) Artificial neural networking (ANN) analysis for heat and entropy generation in flow of non-Newtonian fluid between two rotating disks, *Math. Method Applied Sci*, <https://doi.org/10.1002/mma.7310>